Epithelial Tissues as Active Solids: From Nonlinear Contraction Pulses to Rupture Resistance

Shahaf Armon[1], Matthew S. Bull[2], Avraham Moriel[3], Hillel Aharoni[1], Manu Prakash[4]

1. Department of Physics of Complex Systems, Weizmann Institute of Science, Rehovot, Israel
2. Department of Applied Physics, Stanford University, California, USA
3. Department of Chemical and Biological Physics, Weizmann Institute of Science, Rehovot, Israel
4. Department of Bio-Engineering, Stanford University, California, USA

Corresponding author: shahaf.armon@weizmann.ac.il

Keywords: Epithelium mechanics, contraction pulses, trigger waves, mechanical feedback, active solid, tissue integrity, active cohesion, Trichoplax (Placozoa).

Abstract:

Epithelial tissues in many contexts can be viewed as soft active solids. Their active nature is manifested in the ability of individual cells within the tissue to contract and/or remodel their mechanical properties in response to various conditions. Little is known about the emergent properties of such materials. Specifically, how an individual cellular activity gives rise to collective spatiotemporal patterns is not fully understood. Recently we reported the observation of ultrafast contraction pulses in the dorsal epithelium of *T.adhaerens* in vivo [1] and speculated these propagate via mechanical fields. Other accumulating evidence suggest mechanics is involved in similar contractile patterns in embryonic development in vivo and in cellular monolayers in vitro. Here we show that a widespread cellular response – activation of contraction in response to stretch – is sufficient to give rise to nonlinear propagating contraction pulses. Using a minimal numerical model and theoretical considerations we show how such mechanical pulses emerge and propagate, spontaneously or in response to external stretch. The model – whose mathematical structure resembles that of reaction-diffusion systems – explains observed phenomena in *T. adhaerens* (e.g. excitable or spontaneous pulses, pulse interaction) and predicts other phenomena (e.g. symmetric strain profile, "spike trains"). Finally, we show that such an active two-dimensional sheet dynamically distributes external loads across its surface, facilitating tissue resistance to rupture due to cellular strain. Adding a cellular softening-threshold further enhances the tissue resistance to rupture at cell-cell junctions. As cohesion is at the heart of epithelial physiology, our model may be relevant to many other epithelial systems, even if manifested at different time/length scales.

Significance:

Our work demonstrates that many observed dynamical phenomena in epithelial tissues can be explained merely by mechanical cell-cell interactions, and do not require chemical diffusion or transport between cells (though chemical activity may participate in relevant intracellular processes). Specifically, we show that single cell extension-induced-contraction (EIC) is sufficient to generate propagating contraction pulses, which also increase the tissue's resistance to rupture, an essential function of epithelia. Our results may shed light on how epithelial tissues function under challenging physiological conditions, e.g. in lung, gut, vasculature and other biomedical contexts. Our results may also be relevant in the study of early evolution of multicellularity and the nervous-muscular systems. Finally, the work offers guidelines for designing soft synthetic solids with improved mechanical properties.

Introduction:

Epithelial cells form confluent layers and are thus inherently mechanically coupled. In recent years multiple observations are accumulating showing contraction patterns and dynamics in epithelial tissues that are suspected to be governed mechanically. These evidence include contraction fronts in drosophila embryo during development [2] and density waves in MDCK cell monolayers in-vitro, either in confinement [3, 4], during expansion [4, 5] or under substrate-shear [6]. Theoretical works suggest models to explain the contractile patterns [7–11], models that include mechanical alongside chemical fields, diffusion or active transport. Note, that all these systems, and the suggested models, exhibit dynamics in time scales of minutes to hours.

Recently we reported the observation of ultrafast contraction dynamics in the dorsal epithelium of *T. adhaerens*, including traveling pulses that propagate across the entire animal [1]. The pulses are seen while the animal is freely moving. The propagating pulses initiate spontaneously, not regularly, propagate at a speed of 1-3 cells per second (10-30um/sec), and transmit a contraction of about 50% in cell area in 1 second (Fig1a-c). These contraction waves can propagate uniaxially, split at the propagating fronts and annihilate themselves. Importantly, this early-divergent animal has no reported muscles, neurons or synapses, and its epithelium has no gap junctions that can support cell-cell transport. In addition, since the propagation speeds are extremely fast, it excludes slower processes (such as transcription) from being involved. All these raise the speculation that mechanics governs the contraction propagation.

T. adhaerens is an ideal system to investigate epithelium dynamics. The thin, flat, suspended monolayer resembles early embryonic tissues not only in its minimal components (lacking extra cellular matrix and basement membrane) but also in its large strains dynamics (both individual cells and the entire body undergo dramatic shape changes constantly) [1]. However, unlike embryonic tissues, which undergo slow, stereotypical deformations in time scale of minutes to hours, contraction pulses in the dorsal epithelium of *T. adhaerens* propagate in time scale of seconds, in what seems to be part of a physiological/responsive behavior: due to the animal's erratic, locally-driven ciliary locomotion, the tissue is found constantly under alternating tensile/compression stresses [1]. In very large animals the *ventral* epithelium, that does not show contraction behavior, does fracture [12].

The main candidate to be involved in such fast contraction dynamics is Calcium. While Calcium is known to immediately activate actomyosin contractions in neurons and muscles, less is known about calcium signaling in epithelia [13]. Nevertheless "calcium waves" have been observed in various epithelial systems, such as drosophila embryo imaginal disc during development [13, 14] and mammalian cornea, in response to mechanical stress or injury [15, 16]. These waves refer to propagation of high cytoplasmic calcium levels from cell to cell via gap junctions. However, the hierarchy between chemical, mechanical and electrical signals is not entirely clear, as mechano-sensitive Calcium channels are known to be involved [15, 17].

In live, behaving *T. adhaerens* we showed [1] that increasing intracellular calcium levels (by adding the drug Ionomycin to the media) yields simultaneous contractions of all cells to ~ 50% area within seconds [1]. Hence, it is likely that the spontaneous contractions involve calcium as well. However, it is unclear how one contraction triggers the other during a contraction pulse in an early animal that lacks synapses or gap junctions [18]. Diffusion of neuro-peptides in the surrounding water was suggested to coordinate ciliary beating in the ventral tissue of this animal [19], but chemical diffusion is not likely to govern the contraction pulses in the dorsal epithelium, due to the nature of their propagation (uniaxial propagation, front split, pulses annihilation etc).

Here we propose a mechanical model for inter-cellular transmission of contraction in epithelia. The model is based solely on the common single-cell response of Extension-Induced Contraction (EIC). Various experimental evidence have shown such responses in different systems, and different molecular mechanisms have been proposed to participate in it [4, 20–28]. These include mechanosensitive Calcium channels, ERK protein activation, actin alignment, myosin recruitment, conformational changes in adherens junction and more. The diversity of mechanisms for EIC generation hints about its possible evolutionary advantages. We frame our model regardless of the specifics of these intra-cellular processes, and suggest that cellular EIC may be the only requirement for contraction propagation. As such, our model may be relevant to many epithelial systems.

We present numerical and analytical results for tissue contraction dynamics emerging from cellular EIC. Primarily, we write scaling laws for contraction pulses, map its different modes in parameter space, and show that the dynamic patterns are governed by reaction-diffusion type of equations. The model may explain many phenomena seen in *T. adhaerens,* such as single or repeated pulses, either oscillatory or irregular and pulse annihilation. We utilize the model to predict effects that should be confirmed experimentally, including fixed pulse amplitude and symmetric pulse profile.

Lastly, a surprising outcome of our model is the emerging enhanced resistance to rupture in such active materials. We show that the contractile dynamics resulting from EIC support tissue cohesion, as it evenly distributes external loads throughout the surface, reducing high strain values. Note, that this homogenization consumes cellular energy. Also note, that the even strain distribution increases the stresses at cell-cell junctions. In addition, it has been shown in various epithelial systems that the cell cytoskeleton responds to mechanical stretch not only by stiffening/contraction (EIC), but also by softening/yielding [28–32]. How do these antagonist trends interplay is still unknown. By numerically introducing a cell softening response to our model (on top of EIC) we further enhance cohesion, by eliminating high stress values at the junctions. Together, the two cellular responses simultaneously prevent tissue failure in a process we name “active cohesion”.

Results:

We begin by looking at the recently-measured contraction profile in *T. adhaerens* [1] (fig1c). The profile shows the strain evolution of a single cell during a single contraction event (as averaged from multiple cellular events that did not propagate as pulses in the tissue). On average, during such a contraction event, cell area increases gradually to a critical point, at which it abruptly decreases to about half its initial value. Finally, the cell relaxes slowly towards its initial area. Despite the overdamped conditions, the contraction reaches significantly below the cell’s steady state size (“overshoot”). This shows that the contraction is an active process (that consumes internal cell energy) and suggests it includes a force and time scales that are different from the viscoelastic ones. As the contraction seem to happen at some critical cell size, an additional scale is required, to describe the extension needed for activation. These three parameters are the minimal requirements for the model.

We therefore model a single cell as an overdamped elastic entity (rest length l_0, elastic modulus k, media viscosity γ) that is connected in parallel to an active contractile unit (fig1d). The active unit is realizing a simple EIC, using the three scales discussed above: when the cell reaches a critical length l_c, it immediately applies a fixed compression force F_c for a duration of T_c (see discussion for further reasoning and alternative options, see methods for implementation). Inspired by *T. adhaerens* data, we take the active forces to be larger than the elastic force at criticality ($F_c > kl_c$) and the active time scale shorter than the passive one ($T_c < k/\gamma$). Finally, we assume the spring to be linearly elastic: effects of cell-volume conservation, though shown irrelevant to the thin, soft tissue of *T. adhaerens* [1], may require additional nonlinearities.

The mechanical circuit proposed in fig 1d can be found in one of two modes: an *excitable mode*, i.e. contract only in response to external stretch (that is when $l_c > l_0$), or in an *oscillatory mode*, i.e. oscillate spontaneously without any external stimulation, as a relaxation oscillator (that is when $l_c < l_0$)(fig1e). Such an isolated-cell behavior can be mathematically described in a piecewise manner (fig 1D, SI1).

We now examine the emergent behavior of a finite 1D chain of such cells (fig1f). Each cell is a spring connected in parallel to the active-contractile unit, all experiencing viscous drag from the media. Cell-cell junctions are the nodes, that feel tension due to forces from the nearest cells. Throughout our investigation we choose a finite yet large number of cells, N, and free boundaries, in order to imitate *T. adhaerens*, (details in SI2).

First, we consider a chain of N identical excitable cells (i.e. $l_c > l_0$). Initiating all cells at length l_0, the chain will remain at rest. We now introduce an initial stretch, by initiating a rim-cell at $l_i = l_c + \varepsilon$, after which it is set free. The dynamics starts as the stretched cell actively contracts, stretching the next cell in line, due to the spatial coupling in the overdamped conditions. If the induced stretch is sufficient, it triggers another active contraction, and so forth. A contraction pulse then propagates throughout the tissue at a constant speed, v (fig2a-b). The emerging longitudinal perturbation is not an acoustic (inertial) wave, but a slower, trigger-wave in an excitable media, that consumes ATP.

The symmetric shape of the strain signal (fig2b-c) may be surprising, as we defined an asymmetric EIC profile for the individual cell: the expansion induces a much larger contraction. In fact, a cell participating in a contraction pulse shows a symmetric strain profile, with a delayed, reduced shrinkage. To understand this emerging effect, let us examine the pulse propagation at the bulk of this large, deeply overdamped tissue. We notice that essentially the only nodes moving are the ones at the interface between active and passive cells - all other nodes are at rest due to force balance. Therefore, at the interface, the sum of the active and passive cell lengths is fixed. Thus, the dynamics in time of a bulk-cell is as follows: (i) starts at l_0 (ii) gets stretched by its active neighbor to exactly l_c, and gets activated (iii) contracts until reaching l_0, at which point its passive neighbor reaches exactly l_c and gets activated (iv) our cell keeps applying contraction forces without changing its length, as both its neighbors are also active (v) only when an active neighbor deactivates at T_c and starts to relax - our cell finally shrinks, until reaching T_c itself. As a result, the emergent pulse in the tissue is composed of an extension front, followed by an identical (but opposite-sign) contraction front, and in between, all cells are actively contracting yet remain at their rest-length (fig2a-c, mov1).

Hence, in order to derive a simple scaling for the pulse behavior, as a first approximation, we consider two cells with fixed boundaries (this is practically the case at the interface between active and passive cells). By calculating the time it takes for one cell, contracting with F_c, to excite its neighbor (SI2), we estimate the propagation speed of the pulse $v \cong \frac{F_c l_0}{\gamma(l_c - l_0)}$, its width $w \cong vT_c$ and its amplitude $amp \cong 2(l_c - l_0)$. We also find the width of the expansion and contraction peaks to be $\sim\frac{\gamma}{k}$. Our numerical results confirm all these scaling laws (fig 2h-k).

We use the derived scaling to find the requirements for pulses to appear: The initial stretch should excite the first cell ($l_i > l_c$), and the impulse of active contraction should be large enough to excite the next cell. Using a set of 3 non-dimensional parameters - normalized time $\tilde{t} = \frac{T_c k}{\gamma}$, normalized force $\tilde{f} = \frac{F_c}{k l_c}$, and normalized strain $\tilde{\epsilon} = \frac{l_c - l_0}{l_0}$ - this requirement estimates to $\tilde{t} > \frac{\tilde{\epsilon}}{\tilde{f}}$ (SI2). When the system satisfies these criteria, a pulse propagates indefinitely in the tissue with fixed speed. In the absence of these requirements, the initial stretch decays, and bulk cells stay at their rest lengths indefinitely.

Interestingly, we notice that changing the contraction parameters F_c, T_c changes the pulse velocity v and width w, but not the amplitude, amp (fig2d-e). Only by changing l_c the amplitude is altered (fig2f). As a result, for a given set of activation parameters (l_c, F_c, T_c), if the external stimulation lasts longer than T_c (in our case, if the initial excitation, l_i, is large enough), it generates a "spike train" of several adjacent pulses, all carrying the same quanta of strain - amp (fig 2g, SI2). This effect resembles action potential rate encoding behavior in neural networks [33, 34].

Next, we consider a row of N identical oscillatory cells ($l_c < l_0$). All cells are initiated at l_0 and the boundaries are set to be free. Each cell is a relaxation oscillator, that would beat spontaneously in isolation. However now the cells are additionally subjected to forces coming from their neighbors. We show, that for a wide range of parameters, a mode of ordered pulsations emerges: Initially, all cells contract in a transient irregular phase. Eventually, the system reaches a dynamic steady state (at T_{ss}) where contraction pulses are initiated repeatedly and regularly at the edges and annihilate at the center (fig3a-b, mov2). Annihilation can be seen as a result of the shrinkage front- a "recovering" regime at the back of the pulse that makes the tissue harder to excite (again resembling the refractory period of a neuronal action potential). The annihilation point varies by choosing random initial cell-lengths. The overall tissue length $L(t)$ shrinks from $L(t_0) = N * l_0$ to a steady-state size (L_{ss}) and oscillates around it with amplitude Amp and multiple frequencies $\tau_{1,2,3}$ (fig 3c).

In this mode, cells in the bulk (far from both rim and annihilation points) are effectively fixed at a compressed size: due to viscosity and the large number of cells, the time scale for relaxation is much longer than the typical interval between pulses. Therefore, the pulses propagate through a still and uniform background of cells, that are all at $l \sim l_{ss} < l_c$. As a result a pulse propagates at a fixed speed. Rim cells are the least constrained and hence relax the fastest after a contraction. When they reach criticality, they initiate a new pulse. The pulse profile features are the same as in the excitable mode. The way the system parameters $(l_c, F_c, T_c, k, \gamma, N)$ relate to the emergent measurables (L_{ss}, T_{ss}, v, Amp, $\tau_{1,2,3}$) is plotted from our numerical results in fig3d-e and more elaborately in sfig1. Interestingly, most measurables are invariant to the system size (except T_{ss} and $\tau_{2,3}$), hence are effective "material parameters".

Other solutions exist in the oscillatory mode, aside the ordered pulsations, as shown in the phase diagram (fig3f): when the contraction force is weaker than the elastic retraction at l_c (i.e. $F_c < kl_c$) the system will be "stuck", i.e. continuously apply compression forces but exhibit fixed cell size, that is above l_c. These states may look "flickering" with local activation/deactivation close to criticality (mov3). When the active force is too high, we reach a non-physical regime of the model where cells collapse to negative size (in reality, nonlinear elasticity at the limit of compressibility will prevent that). When the viscosity is high, the time it takes to reach steady state is very long, hence in realistic time scales the dynamics may look irregular. Finally, when viscosity is low, irregular pulsations emerge, as a result of various elastic modes that are not overdamped (mov3). The sharp transition between the regular and irregular traveling pulsations is depicted in fig 3g – as a transition from perfect limit cycles to "smeared" chaotic activity.

Finally, we use the same principles of EIC in a 2D vertex model (which is the common modeling approach for cellular sheets, as opposed to springs models). 2D vertex models are controlled by 5 non dimensional parameters [35–37] – a parameter space which we do not examine completely here. However, we do focus on a regime that we believe is most relevant to *T. adhaerens* (low area stiffness k_A, high F_c , capable of reducing cell area by 50%, and $5T_C \sim \frac{\gamma}{k}$). We consider a disk-like shape of a tissue with free boundaries (fig1g). For the single cell rest-shape we choose a regular, compatible hexagon, with rest perimeter P_0 and rest area A_0 ($A_0 = 3\sqrt{3}\,(P_0/6)^2/\,2$). The cell's perimeter is

controlled by an active unit: when reaching a critical area A_c, a compression force F_c is acting for a duration of T_c to shorten the perimeter (see methods).

The results are qualitatively similar to the 1D case: In the excitable mode case ($A_0 < A_c$), a single pulse is propagating from an initially-perturbed point across the tissue. Note, that the pulse propagates faster closer to the rim (mov4). In the oscillatory mode ($A_c < A_0$), after an initial shrinking phase, the system is self-compressed and contraction pulses are propagating in a uniaxial, azimuthal or a spiral fashion (fig4a, mov5). As in 1D, an expansion front is a precursor to a shrinkage front, while all cells in between are actively contracting. Flickering but mostly contracting modes exist as well, resembling similar states in the 1D case (mov7).

The emergent dynamics we observe take the schematic shape of reaction-diffusion in the displacement vector, $\bar{u}$. This can be seen from a simple continuum model written in the spirit of the discrete model we presented here (SI3). The dynamics may be written as: $\partial_t \boldsymbol{u} = \boldsymbol{D}\nabla^2\boldsymbol{u} + \boldsymbol{R}$ where the diffusion coefficient depend on viscoelasticity $|\boldsymbol{D}| = k/\gamma$ and the reaction term, $\boldsymbol{R}$, depends on the cellular activity.

Despite the similarities to the 1D setting, a unique feature of the 2D case is the fact the system is prone to mechanical frustration. An intuitive way to see it, is that rim-cells can only release stresses in the radial axis, but not in the azimuthal one. As a result, rim-cells are not beating like isolated cells, as in 1D. Although rim-cells relax faster than bulk cells, they still need to "wait" for the entire system to relax before they can too, as seen in the radial gradient of strain (mov6,7,sfig2). In addition, bulk cells are relaxing slowly due to viscosity and due to the energy wells they reach at concave shapes (their perimeter needs to temporarily decrease in order to go back to convexity). The result is long intervals of quiescence. We show that as $\tilde{f}$ increases, quiescence periods increase, while short bursts of activity occur between them (sfig2).

An intriguing feature of this 2D active tissue is its effective mechanical properties under tensile stress. To demonstrate it, we design a numerical experiment where we pull a 2D sheet at two opposite rim points with a constant force (fig4d). A passive elastic material yields high values of strain, focused near the pinching points (at steady state – the spatial distribution decays as a power law) (fig 4Ei). A viscoelastic material pulled in the same way would either postpone the same steady state or create indefinite creep (depending on the specific model used) both effects impose a threat for tissue cohesion. However, pulling on the active tissue results in a more even strain distribution. Although the resulting steady state is dynamic, peak strains are evenly distributed in space (fig 4Eii). This can be seen also in the strain values histogram of all data points (fig4F): the strain distribution is symmetric around zero, with a minimal tail of high strain values. This effect reduces the chances for rupture due to cell strain, at the cost of high stress values in the cell-cell junctions.

We show that adding a second cellular response - cell yielding due to junction stress - reduces both maximal junctional stresses and cell strain simultaneously. We add to the simulation a cell softening threshold- decrease in the elastic module by factor 2 upon reaching critical junction stress σ_s (fig 4B, methods). The added response does not change the spatiotemporal patterns significantly, except introducing a tailing softening pulse (fig4C, mov6). The second threshold also did not change the strain and stress distributions dramatically, but it did cut-off high stress values, trading them for localized high strains, as seen in the trade-off at the distribution tails (fig 4Eiii,F). If the two thresholds (A_c, σ_s) are set below rupture values, the tissue can avoid failure by suppressing both cell strain and junction stress simultaneously.

Discussion

We suggest a model for propagation of contraction pulses in epithelia. Pulse propagation is a direct result of a single cell EIC- contraction due to extension. Unlike passive elastic retraction after extension, the model requires the contraction to be active, and include a "memory" time scale, in order to bring a contracting cell significantly below its rest length at the overdamped conditions. We show that in order for a contraction to propagate in the excitable-cell mode, the contraction impulse should be strong enough relative to the excitation threshold $\tilde{tf} > \tilde{\epsilon}$ (a qualitatively similar criterion will exist in the oscillatory-cell mode, with l_{ss} in the role of l_0). The resulting pulses travel in the excitable media via local energy injections, and evolve dynamically following reaction-diffusion equations for the strain.

In actual biological tissues, it is unclear whether an EIC is triggered by strain, stress or strain rate. The exact parameter is hard to distinguish experimentally, and is currently unknown. For our model, we choose cell-strain and junction-stress as triggers, as they threat tissue cohesion: cell cortex networks rearrange due to stress, but are probable to fail entirely in high strain. Cell-cell junctions, on the other hand, do not "expand", but may break under stress. In addition, in the presence of drag, a cellular contraction reduces cell strain but increases junction stress. Therefore, we choose high cell strain as the trigger for contraction and high junction stress as the trigger for softening. We claim these feedback loops promote tissue stability.

We choose the active contraction to be governed by a fixed compression force that lasts a fixed duration of time. This is a minimal assumption inspired by our experimental results from *T. adhaerens*, where we showed the single contraction profile, as well as a narrow distribution of contraction times relative to contraction amplitudes and speeds [1]. Nevertheless, other functional behavior of contraction that brings the cell to a new, shrunk size at relevant time scales would create contraction pulses that are qualitatively similar.

We propose a new physiological role for contractility in epithelia: rupture resistance. As EIC is a common epithelial response, and as tissue integrity is at the heart of any epithelium function, "active cohesion" may be relevant in a wide range of systems, even if manifested in different time and length scales. The minimal nonlinear model we presented fits the fast soliton nature of the pulses seen in *T. adhaerens* but may be applicable to other observed contraction waves in epithelia (as in drosophila embryo and MDCK monolayers). This hypothesis should be further tested experimentally. Specifically, it would be interesting to test it in various embryonic tissues, and in epithelia that is either contractile or prone to high, repeatable mechanical stresses (e.g. heart, lung, gut, bladder, vasculature).

Our work brings forward discrete aspects of tissue mechanics, such as cellular chemical thresholds, local mechanical conditions under cell contractility and preferred cellular geometry. It would be interesting to compare discrete, continuous and hybrid models, to describe observed phenomena in epithelial tissues.

The study of *T. adhaerens* and other early-divergent animals brings tissue-mechanics to the context of evolution of multicellularity. Alongside the fundamental ability of cells to stay cohesive as tissues, it may shed light on the origin of the excitation-contraction coupling and the nervous-muscular system [18]. We suggest to further investigate dynamics in early-epithelia not only in the context of "active cohesion", but also as possible embodied calculations yielding "behavior" and supporting physiological needs (e.g. locomotion and navigation, wound healing and size control). Finally, this work may inspire engineering of synthetic materials that actively resist rupture.

Methods

Simulation code was written in MATLAB (MathWorks, 2017b) and is available on GitHub.

We adopt a dynamical modeling paradigm built around gradient-descent on overdamped equations of motion. Unlike conventional use of gradient descent, the energy functional in the algorithm is not constant; rather, it changes every time a cell is activated or deactivated. Inspired by *T. adhaerens*, we take the activation time T_c to be shorter than the viscoelastic time k/γ, which is the time scale to approach steady state. Therefore, our gradient descent algorithm will not necessarily reach steady state, and indeed in most interesting cases it does not.

The equation of motion is therefore

$$\gamma \dot{l}_i = -\frac{\partial E}{\partial l_i}$$

where l_i is the length of cell #i, and the overall free energy E is a sum of the energies of all cells, $E(t) = \sum_i \varepsilon_i(t)$. (Note that the cellular energy ε_i is different than the cell strain ϵ_i mentioned earlier). In 1D, the energy of each cell is given by

$$\varepsilon_i(t) = k(l_i(t) - l_o)^2 - F_i^{l_c}(t) l_i(t)$$

where the boxcar function $F_i^{l_c}$ represents the cellular contraction forces: $F_i^{l_c}$ takes the value F_c when $l_i > l_c$ and maintains it for a duration of T_c, after which it goes back to 0 (fig1d).

To model 2D tissues, we generalize the above framework using a 2D vertex-model, evolving under the cellular energy function

$$\varepsilon_i = k_A(A_i(t) - A_o)^2 + k_p(P_i(t) - P_0)^2 + F_i^{A_c}(t) P_i(t).$$

The function $F_i^{A_c}$ now takes the value F_c when $A_i > A_c$ and maintains it for a duration of T_c. Note that the force is triggered by an area threshold but acts on the perimeter.

To model tension-induced yielding we add a second cellular response – softening of all cells adjacent to an overstressed junction. The energy functional then becomes:

$$\varepsilon_i = k_A(A_i(t) - A_o)^2 + k_{P,i}(P_i(t) - P_0)^2 + \mathrm{F}_i^{A_c}(t) P_i(t)$$

where $k_{P,i} = k_P$ if the junctions adjacent to the ith cell are all under the critical tension σ_s, and $k_{P,i} = k_s < k_P$ if one of the adjacent junctions is overtensed (see supplementary methods for the exact criterion). In the numerical experiments presented here we choose $k_s = k_P/2$.

Contributions: Designed the research: SA, MSB, MP; Wrote the simulations: MSB; Performed the numerical experiments: SA, MSB; Analyzed the data: SA; Wrote the scaling for contraction pulses: HA. Wrote the continuum model: AM; Wrote the manuscript: SA; Supervised the project: MP.

Acknowledgements: We thank Elisha Moses, Sam Safran, Eran Bouchbinder, Nir Gov and Efi Efrati for useful discussions and comments. We acknowledge financial support from the Weizmann Institute of Science -Women Bridge Position and the Israeli Ministry of Absorption New Immigrant funds to S.A, Horwitz Research grant and the Center for New Scientists at the Weizmann Institute for HA, NIH Innovators award, HHMI Faculty Fellows Program, NSF CCC award and CZI BioHub Investigator funds to M.P.

References

1. Armon S, Bull MS, Aranda-Diaz A, Prakash M (2018) Ultrafast epithelial contractions provide insights into contraction speed limits and tissue integrity. Proc Natl Acad Sci U S A 115:E10333–E10341. https://doi.org/10.1073/pnas.1802934115

2. Bailles A, Collinet C, Philippe J-M, et al (2019) Genetic induction and mechanochemical propagation of a morphogenetic wave. Nature 572:467–473. https://doi.org/10.1038/s41586-019-1492-9

3. Peyret G, Mueller R, d'Alessandro J, et al (2019) Sustained Oscillations of Epithelial Cell Sheets. Biophys J 117:464–478. https://doi.org/10.1016/J.BPJ.2019.06.013

4. Hino N, Rossetti L, Marín-Llauradó A, et al (2019) ERK-mediated mechanochemical waves direct collective cell polarization. bioRxiv 2019.12.25.888552. https://doi.org/10.1101/2019.12.25.888552

5. Serra-Picamal X, Conte V, Vincent R, et al (2012) Mechanical waves during tissue expansion. Nat Phys 8:628–634. https://doi.org/10.1038/nphys2355

6. Sadeghipour E, Garcia MA, Nelson WJ, Pruitt BL (2018) Shear-induced damped oscillations in an epithelium depend on actomyosin contraction and E-cadherin cell adhesion. Elife 7:. https://doi.org/10.7554/eLife.39640

7. Banerjee S, Utuje KJC, Marchetti MC (2015) Propagating Stress Waves During Epithelial Expansion. Phys Rev Lett 114:228101. https://doi.org/10.1103/PhysRevLett.114.228101

8. Dierkes K, Sumi A, Solon J, Salbreux G (2014) Spontaneous Oscillations of Elastic Contractile Materials with Turnover. Phys Rev Lett 113:148102. https://doi.org/10.1103/PhysRevLett.113.148102

9. Boocock D, Hino N, Ruzickova N, et al (2020) Theory of mechano-chemical patterning and optimal migration in cell monolayers. bioRxiv 2020.05.15.096479. https://doi.org/10.1101/2020.05.15.096479

10. Blanchard GB, Étienne J, Gorfinkiel N (2018) From pulsatile apicomedial contractility to effective epithelial mechanics. Curr Opin Genet Dev 51:78–87. https://doi.org/10.1016/J.GDE.2018.07.004

11. Lin S-Z, Li B, Lan G, Feng X-Q (2017) Activation and synchronization of the oscillatory morphodynamics in multicellular monolayer. Proc Natl Acad Sci 114:8157–8162. https://doi.org/10.1073/PNAS.1705492114

12. Prakash VN, Bull MS, Prakash M (2019) Motility induced fracture reveals a ductile to brittle crossover in the epithelial tissues of a simple animal. bioRxiv 676866. https://doi.org/10.1101/676866

13. Balaji R, Bielmeier C, Harz H, et al (2017) Calcium spikes, waves and oscillations in a large, patterned epithelial tissue. Sci Rep 7:42786. https://doi.org/10.1038/srep42786

14. Wu Q, Brodskiy PA, Huizar F, et al (2017) In vivo relevance of intercellular calcium signaling in Drosophila wing development. bioRxiv 187401. https://doi.org/10.1101/187401

15. D'hondt C, Himpens B, Bultynck G (2013) Mechanical Stimulation-induced Calcium Wave Propagation in Cell Monolayers: The Example of Bovine Corneal Endothelial Cells. J Vis Exp e50443. https://doi.org/10.3791/50443

16. Chifflet S, Justet C, Hernández JA, et al (2012) Early and late calcium waves during wound healing in corneal endothelial cells. Wound Repair Regen 20:28–37. https://doi.org/10.1111/j.1524-475X.2011.00749.x

17. Frame MK, de Feijter AW (1997) Propagation of Mechanically Induced Intercellular Calcium Waves via Gap Junctions and ATP Receptors in Rat Liver Epithelial Cells. Exp Cell Res 230:197–207. https://doi.org/10.1006/EXCR.1996.3409

18. Mackrill JJ, Shiels HA (2020) Evolution of Excitation-Contraction Coupling. Springer, Cham, pp 281–320

19. Senatore A, Reese TS, Smith CL (2017) Neuropeptidergic integration of behavior in Trichoplax adhaerens, an animal without synapses. J Exp Biol 220:3381. https://doi.org/10.1242/JEB.162396

20. Odell GM, Oster G, Alberch P, Burnside B (1981) The mechanical basis of morphogenesis. I. Epithelial folding and invagination. Dev Biol. https://doi.org/10.1016/0012-1606(81)90276-1

21. Fernandez-Gonzalez R, Simoes S de M, Röper J-C, et al (2009) Myosin II Dynamics Are Regulated by Tension in Intercalating Cells. Dev Cell 17:736–743. https://doi.org/10.1016/J.DEVCEL.2009.09.003

22. Clemen AE-M, Vilfan M, Jaud J, et al (2005) Force-Dependent Stepping Kinetics of Myosin-V. Biophys J 88:4402. https://doi.org/10.1529/BIOPHYSJ.104.053504

23. Norstrom MF, Smithback PA, Rock RS (2010) Unconventional Processive Mechanics of Non-muscle Myosin IIB. J Biol Chem 285:26326. https://doi.org/10.1074/JBC.M110.123851

24. Noll N, Mani M, Heemskerk I, et al (2017) Active Tension Network model suggests an exotic mechanical state realized in epithelial tissues. Nat Phys 13:1221. https://doi.org/10.1038/NPHYS4219

25. Mulla Y, MacKintosh FC, Koenderink GH (2019) Origin of Slow Stress Relaxation in the Cytoskeleton. Phys Rev Lett 122:218102. https://doi.org/10.1103/PhysRevLett.122.218102

26. Heisenberg C-P, Bellaïche Y (2013) Forces in Tissue Morphogenesis and Patterning. Cell 153:948–962. https://doi.org/10.1016/j.cell.2013.05.008

27. Heer NC, Martin AC (2017) Tension, contraction and tissue morphogenesis. Development 144:4249. https://doi.org/10.1242/DEV.151282

28. Banerjee S, Gardel ML, Schwarz US (2020) The Actin Cytoskeleton as an Active Adaptive Material. Annu Rev Condens Matter Phys 11:421–439. https://doi.org/10.1146/annurev-conmatphys-031218-013231

29. Khalilgharibi N, Fouchard J, Asadipour N, et al (2019) Stress relaxation in epithelial monolayers is controlled by the actomyosin cortex. Nat Phys 15:839–847. https://doi.org/10.1038/s41567-019-0516-6

30. Latorre E, Kale S, Casares L, et al (2018) Active superelasticity in three-dimensional epithelia of controlled shape. Nature 563:203–208. https://doi.org/10.1038/s41586-018-0671-4

31. Chaudhuri O, Parekh SH, Fletcher DA (2007) Reversible stress softening of actin networks. Nature 445:295–298. https://doi.org/10.1038/nature05459

32. D'Angelo A, Dierkes K, Carolis C, et al (2019) In Vivo Force Application Reveals a Fast Tissue Softening and External Friction Increase during Early Embryogenesis. Curr Biol 29:1564-1571.e6. https://doi.org/10.1016/J.CUB.2019.04.010

33. Azarfar A, Calcini N, Huang C, et al (2018) Neural coding: A single neuron's perspective. Neurosci Biobehav Rev 94:238–247. https://doi.org/10.1016/J.NEUBIOREV.2018.09.007

34. Nordlie E, Tetzlaff T, Einevoll GT (2010) Rate dynamics of leaky integrate-and-fire neurons with strong synapses. Front Comput Neurosci 4:149. https://doi.org/10.3389/fncom.2010.00149

35. Bi D, Lopez JH, Schwarz JM, Manning ML (2015) A density-independent rigidity transition in biological tissues. Nat Phys 11:1074–1079. https://doi.org/10.1038/nphys3471

36. Manning ML, Foty RA, Steinberg MS, Schoetz E-M (2010) Coaction of intercellular adhesion and cortical tension specifies tissue surface tension. Proc Natl Acad Sci U S A 107:12517–22. https://doi.org/10.1073/pnas.1003743107

37. Alt S, Ganguly P, Salbreux G (2017) Vertex models: from cell mechanics to tissue morphogenesis. Philos Trans R Soc Lond B Biol Sci 372:. https://doi.org/10.1098/rstb.2015.0520

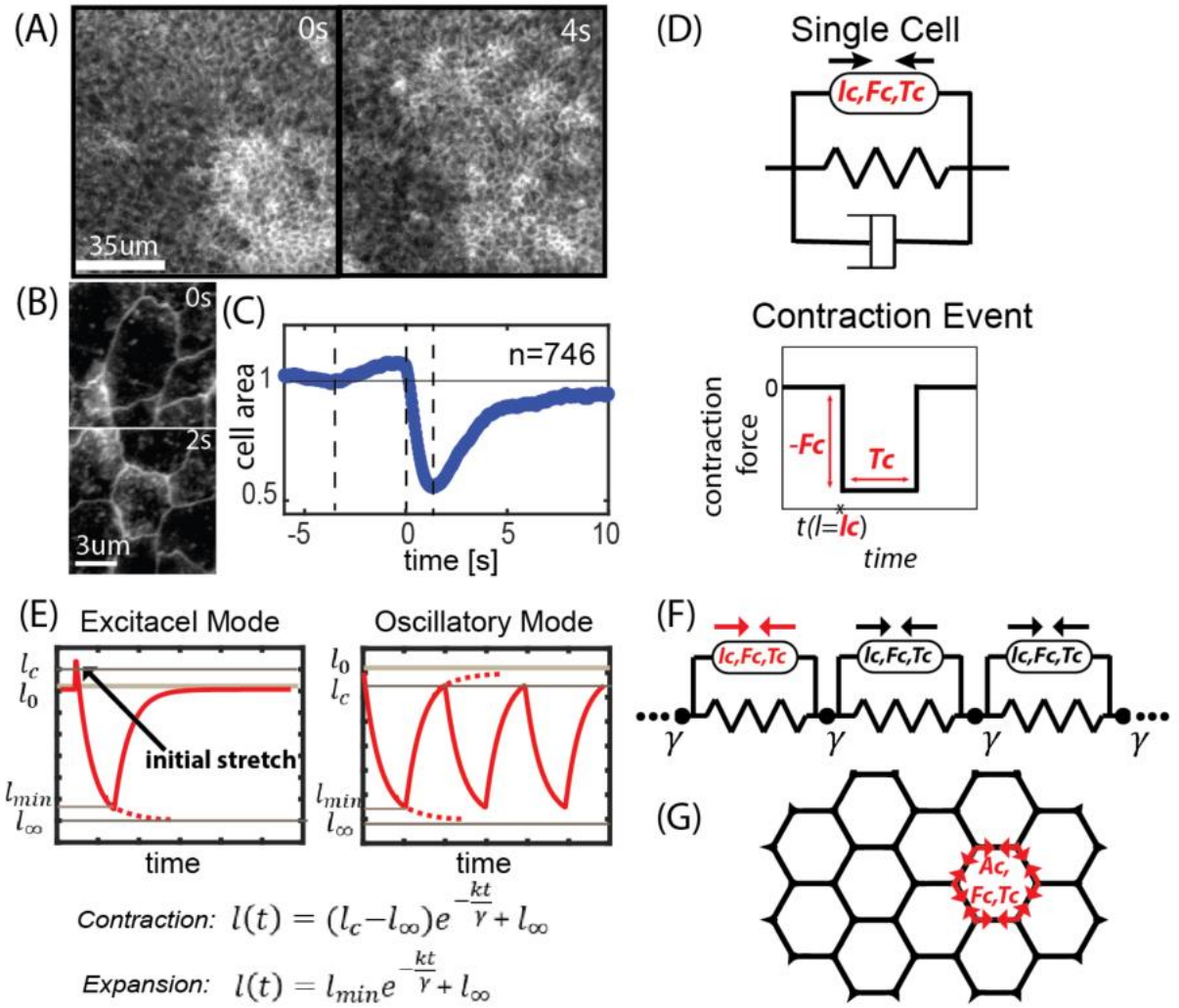

Fig. 1: Modeling epithelium with cellular EIC (extension-induced-contraction): (A-C) Experimental results from contractions in the dorsal epithelium of *T. adhaerens* (reproduced from [1]). (A) Snapshots from contraction pulses in the tissue, imaged using fluorescent membrane stain. (B) Snapshots from a cellular contraction event. The contraction induces expansion of neighboring cells. (C) The average contraction profile of single cells within the tissue (such that are not participating in pulses). (D) The mechanical circuit representing the single cell in our model. The active unit, placed in parallel to the spring, represents the active response: beyond a critical length l_c, a cell contracts with constant force F_c for a given period of time, T_c. In the simulations we use a boxcar function: immediate activation and termination of the force. The cell is found in a media with viscosity γ (E) The behavior of isolated such cells, in either an excitable mode ($l_0 < l_c$), or oscillatory mode ($l_c < l_0$). The piecewise exponential solutions are written below. More details in SI1. (F-G) Sketches of the 1D and 2D settings in our simulations. The degrees of freedom are the vertices between cells that are free to move under cellular forces and viscous drag. The systems are large but finite and the boundary is free.

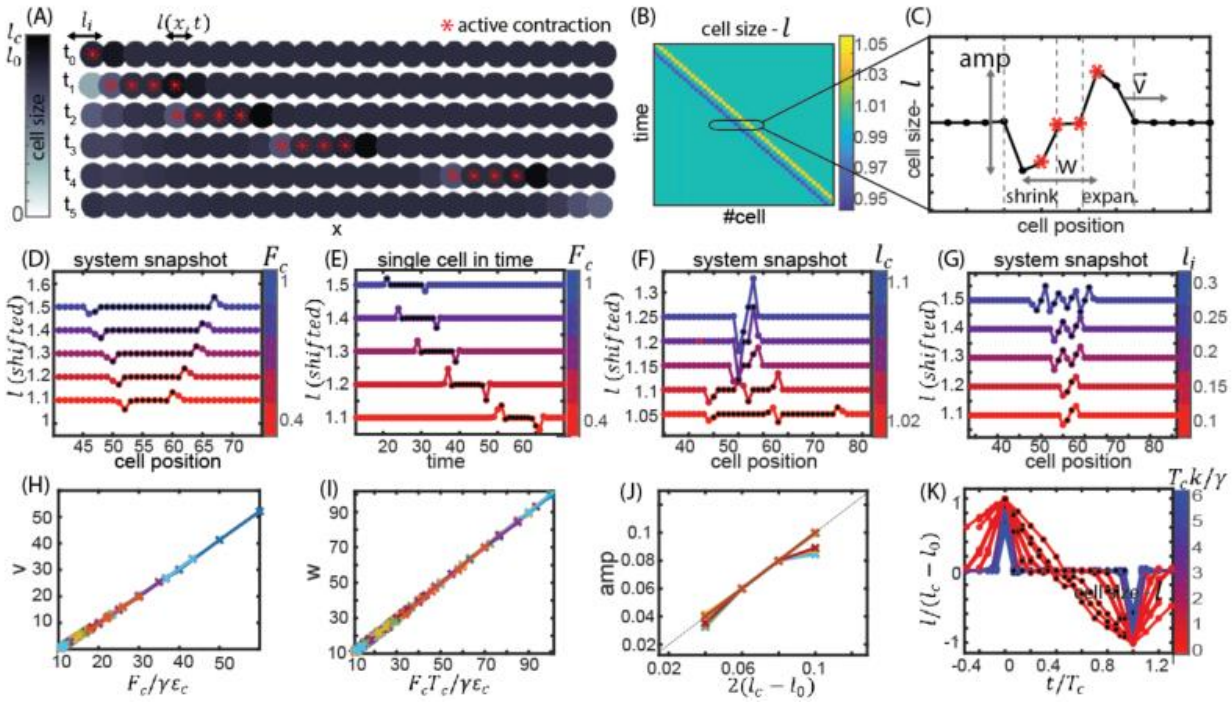

Fig 2: Contraction pulses in a 1D excitable tissue: (A) Snapshots from a dynamic simulation (mov1) of a 1D chain of excitable cells ($l_0 < l_c$) show the propagation of a single contraction pulse from left to right. At t_0 all cells are set at their rest length, l_0, except the first cell on the left, that is initiated at $l_i > l_c$, which triggers the pulse. Greyscale represents cell size; red asters represent activated cells. (B) A kymograph representation of the dynamics shows the pulse propagation in the tissue at constant pulse width, w, and speed, v (defined in units of cells and cells per time, respectively). (C) A section from the kymograph shows the pulse profile: an expansion-front first, and an equal but opposite contraction-front behind it. All cells in between are actively contracting (marked in red asters) yet found at their rest length. (D) System snapshots from simulations with different F_c values. Results show that Increasing F_c increases the pulse's width. (E) Time series of a specific bulk cell taken from the same simulations as (D). Results show that increasing F_c increases the pulse's speed (the pulse reaches the same cell sooner). (F) System snapshots from simulations with different l_c values. Results show that increasing l_c increases the amplitude of the signal. (G) System snapshots from simulations with different l_i values. A "spike train" made of identical pulses is emergent. The number of pulses depends on l_i. (H-K) Using the scaling laws we derived, we show a collapse of the numerical results into known functions of the parameters.

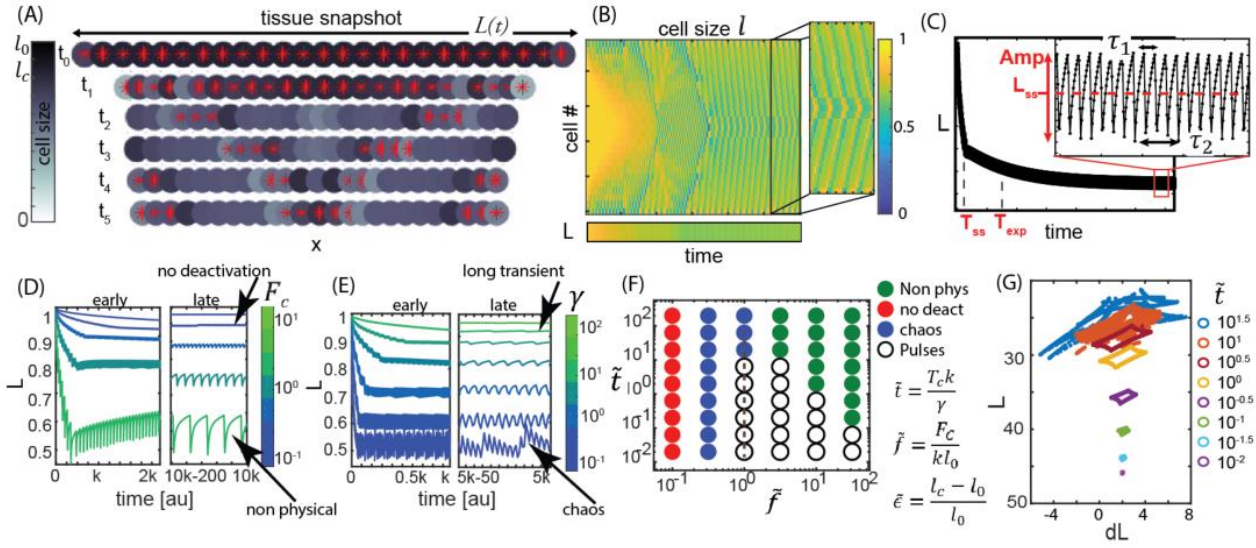

Fig3: Contraction pulses in a 1D oscillatory tissue: (A) Snapshots from a dynamic simulation (mov2) of a 1D chain of oscillatory cells ($l_c < l_0$). At t_0 all cells are set to their elastic rest length l_0. At t_1 the system is at its transient shrinking phase. At t_{2-5} the system is at its dynamic steady state. Contraction pulses are constantly propagating from the edges to the bulk of the tissue, where they collide and annihilate. The overall length fluctuates around L_{ss}. Greyscale represents cell size; red asters represent activated cells. (B) A kymograph representation of the dynamics shows the pulses propagation at constant speed and their annihilating at the center. The bottom bar shows the overall tissue length, L. (C) A sample measurement of $L(t)$. The ordered traveling pulses emerge at T_{ss}. Then, further exponential decay (time scale T_{exp}) brings the system to its asymptotic average length L_{ss}, around which it fluctuates with multiple frequencies. (D-E) Time series of $L(t)$ as F_c and γ vary. We show early and late intervals, taken from long simulation runs. While we focus on ordered pulsatile behavior, different possible types of dynamics are seen at the extremities of parameter space. These include all-contractile ("no-deactivation") mode; cell collapse to negative area ("non-physical"); increasingly long T_{ss} ("long transient"); and irregular traveling pulses ("chaos"). More details in sfig1. (F) A phase diagram shows the different types of dynamics as a function of the non-dimensional parameters $\tilde{f}$and $\tilde{t}$. (G) A sharp transition from an ordered pulsation mode (limit cycles) to chaos as a function of γ. The trajectory in $\tilde{t}$ is depicted in dashed line in (F). Plotted data points are taken from steady-state.

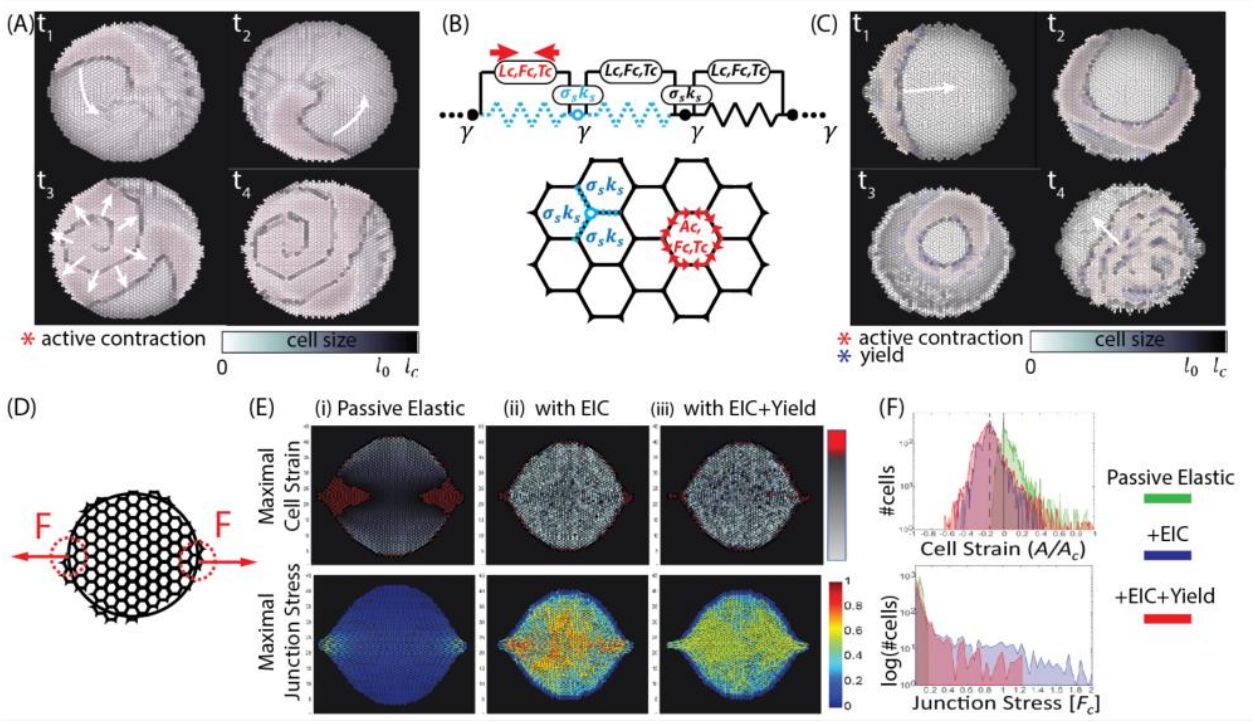

Fig4: 2D Oscillatory tissue: dynamics and "active cohesion" (A) Snapshots from a dynamic simulation of a 2D cellular sheet with EIC (mov 5) shows circular and spiral pulses with features similar to the 1D case: an extension front, followed by a shrinking front, while all cells in between are actively contracting. Greyscale represents cell size; red asters represent activated cells. (B) Adding a second cellular response: When the tension on a cell-cell junction reaches a threshold σ_s– the cell yields. We model that by immediate softening (reduction in the perimeter's elastic modulus k_p by factor 2) in all neighboring cells. (C) Snap shots from a simulation (mov 6) of a tissue with both contraction and softening thresholds. The patterns seem similar to (A), with softening fronts accompanying the extension and shrinkage fronts. (D-F) Testing the tissue's response to external stretch in the x-axis (D) A sketch of the pulling configuration: constant force is pulling uniaxially on the sheet, acting directly on a finite area in each side. (E) We compare a passive material (i), a material with contraction response (mov8) (ii), and one with both contraction and yielding responses (mov9) (iii). We present peak values of cell strain (top) and junction stress (bottom) throughout the simulation. The passive elastic material develops strain and stress focusing near the pulling points (as a fixed steady state). The contractile material dynamically distributes the strains in the tissue but "pays" with high values of junction stress. A material with the added yield response increases slightly the levels of cell strain but cuts-off high junction stress values. (F) Histogram-view of the data in D.